Modern Pathology (2021) 34:672–683
https://doi.org/10.1038/s41379-020-00681-x

ARTICLE

MicroRNA signatures associated with lymph node metastasis in intramucosal gastric cancer

Seokhwi Kim[1] · Won Jung Bae[1] · Ji Mi Ahn[1] · Jin-Hyung Heo[2] · Kyoung-Mee Kim[3] · Kyeong Woon Choi[4] · Chang Ohk Sung[4,5] · Dakeun Lee[1]

Received: 14 April 2020 / Revised: 4 September 2020 / Accepted: 7 September 2020 / Published online: 24 September 2020

Abstract

Although a certain proportion of intramucosal carcinomas (IMCs) of the stomach does metastasize, the majority of patients are currently treated with endoscopic resection without lymph node dissection, and this potentially veils any existing metastasis and may put some patients in danger. In this regard, biological markers from the resected IMC that can predict metastasis are warranted. Here, we discovered unique miRNA expression profiles that consist of 21 distinct miRNAs that are specifically upregulated (miR-628-5p, miR-1587, miR-3175, miR-3620-5p, miR-4459, miR-4505, miR-4507, miR-4720-5p, miR-4742-5p, and miR-6779-5p) or downregulated (miR-106b-3p, miR-125a-5p, miR-151b, miR-181d-5p, miR-486-5p, miR-500a-3p, miR-502-3p, miR-1231, miR-3609, and miR-6831-5p) in metastatic (M)-IMC compared to nonmetastatic (N)-IMC, or nonneoplastic gastric mucosa. Intriguingly, most of these selected miRNAs showed stepwise increased or decreased expression from nonneoplastic tissue to N-IMC to M-IMC. This suggests that common oncogenic mechanisms are gradually intensified during the metastatic process. Using a machine-learning algorithm, we demonstrated that such miRNA signatures could distinguish M-IMC from N-IMC. Gene ontology and pathway analysis revealed that TGF-β signaling was enriched from upregulated miRNAs, whereas E2F targets, apoptosis-related, hypoxia-related, and PI3K/AKT/mTOR signaling pathways, were enriched from downregulated miRNAs. Immunohistochemical staining of samples from multiple institutions indicated that PI3K/AKT/mTOR pathway components, MAPK1, phospho-p44/42 MAPK, and pS6 were highly expressed and the expression of SMAD7, a TGF-β pathway component, was decreased in M-IMC, which could aid in distinguishing M-IMC from N-IMC. The miRNA signature discovered in this study is a valuable biological marker for identifying metastatic potential of IMCs, and provides novel insights regarding the metastatic progression of IMC.

Introduction

With advances in diagnostic surveillance, gastric cancer (GC) is now detected earlier and prognosis is improving. In particular, patients with intramucosal carcinoma (IMC) mostly experience complete cure once the tumor is resected, mainly because this early stage of disease is unlikely to develop metastasis. However, a certain proportion of IMCs do recur and even metastasize to liver and bone as well as regional lymph nodes [1–4]. Previous studies have demonstrated that lymph node metastasis occurs in 1.9–3.5% of IMCs, and some of these patients eventually

Supplementary information The online version of this article (https://doi.org/10.1038/s41379-020-00681-x) contains supplementary material, which is available to authorized users.

✉ Chang Ohk Sung
co.sung@amc.seoul.kr

✉ Dakeun Lee
dakeun@gmail.com

[1] Department of Pathology, Ajou University School of Medicine, Suwon, Korea

[2] Department of Pathology, CHA Bundang Medical Center, CHA University, Seongnam, Korea

[3] Department of Pathology and Translational Genomics, Samsung Medical Center, Sungkyunkwan University School of Medicine, Seoul, Korea

[4] Department of Medical Science, Asan Medical Institute of Convergence Science and Technology, Asan Medical Center, University of Ulsan College of Medicine, Seoul, Korea

[5] Department of Pathology, Asan Medical Center, University of Ulsan College of Medicine, Seoul, Korea

succumb to the disease [3, 5–7]. As most IMCs are now treated with endoscopic submucosal dissection (ESD) rather than by radical gastrectomy, the exact incidence of regional lymph node metastasis in this early stage of disease remains largely unknown. Once a tumor is resected and histologically diagnosed as IMC, it is assumed that there will be no metastasis and the patient will receive no additional adjuvant treatment. Considering that lymph node biopsy or dissection is included in the standardized treatment protocol in cancers of other organs showing similar rates of nodal metastasis [8, 9], this lack of surveillance of nodal status may pose a potential risk of disease progression in such early GC patients.

To overcome this, many researchers have investigated the clinicopathologic factors predicting lymph node metastasis by studying metastatic IMCs (M-IMCs) [3, 5, 6]. According to these previous reports, pathologic features such as large tumor size (usually >2 cm), invasion to the muscularis mucosa, presence of an ulcer, and undifferentiated-type histology are commonly associated with lymph node metastasis in IMC. Despite these efforts, lymph node metastasis is still barely predictable, because most of these cases finally eventuate to be nonmetastatic, even though they exhibit all the above risk factors. Radical gastrectomy with regional lymph node dissection is not regarded as a treatment of choice in patients with IMC, as ESD provides several profound benefits to patients. Thus, identification of new biomarkers that can more precisely predict metastasis in IMC is warranted for tailored therapy.

Over the past decade, multiplexed, high-throughput technologies have enabled numerous fresh human tumor-based genomic sequencing studies, which unmasked certain new oncogenic driver mutations and underlying mechanisms involved in cancer progression or resistance to treatment [10, 11]. However, regarding GC, these studies have been mostly limited to advanced stages of the disease because very early-stage GCs are small and shallow, and are not clearly delineated; thus, fresh tumor sampling is not possible in most circumstances. Therefore, studies investigating the molecular characteristics surrounding IMC have only rarely been conducted, and the underlying mechanisms involved in early-stage cancer metastasis have remained largely elusive.

MicroRNAs (miRNAs) are small noncoding RNAs that are known to regulate gene expression. Through binding to a 3′ untranslated region of a mRNA, which is partially complementary to their target sequence, miRNAs inhibit or promote the translation of various mRNAs of oncogenes or tumor suppressor genes to impact cancer biology. Several studies have been conducted to identify miRNAs that are related to cancer progression or patient prognosis in various types of malignancies [12–15]. Regarding GCs, it has been reported that certain miRNAs are aberrantly expressed in GC [16], and some of these show value in predicting patient prognosis [17]. A recent study revealed distinct miRNA expression profiles that are related to the different stages of gastric carcinogenesis, from nonneoplastic gastric mucosa to adenoma to early GC [18], which underscores the crucial role of miRNAs in the development and progression of cancer. Nevertheless, miRNA profiles specifically related to metastasis in IMC have never been reported.

Here, we investigated unique miRNA expression profiles of M-IMC in comparison to non-M-IMC (N-IMC) and nonneoplastic gastric mucosa. By analyzing the target genes of the identified miRNAs, we elucidated the biological modes of action underlying the progression of M-IMC. Also, with a machine-learning algorithm and immunohistochemical staining, we internally and externally validated the miRNA expression profiles of M-IMC.

Materials and methods

Clinical samples

We reviewed medical records of patients who underwent gastrectomy from July 2005 to March 2012 at Ajou University Hospital, and selected an experimental set which consisted of 7 cases of normal gastric mucosa, 12 cases of N-IMC, and 16 cases of M-IMC. For the independent validation, 108 formalin-fixed, paraffin-embedded (FFPE) samples from three different institutes were selected; 54 cases of M-IMC from Samsung Medical Center (47 cases) and Bundang CHA Hospital (7 cases) and 54 cases of N-IMC samples from Ajou University Hospital were included. This study was carried out following the code of ethics of the World Medical Association (Declaration of Helsinki), and was approved by the Institutional Review Board of Ajou University Hospital (AJIRB-BMR-KSP-17-129).

miRNA extraction and microarray analysis

Total RNA, including miRNAs, was extracted from the FFPE normal and tumor specimens and was prepared using Affymetrix GeneChip miRNA (cat. no. 902412; Affymetrix, Santa Clara, CA, USA), according to the manufacturer's instructions. For quality control, RNA purity and integrity were evaluated by determination of OD 260/280 nm ratio, and analyzed using an Agilent 2100 Bioanalyzer instrument (Agilent Technologies, Palo Alto, CA, USA). One microgram RNA samples were labeled with the FlashTag™ Biotin RNA Labeling Kit (Genisphere, Hatfield, PA, USA). The labeled RNA was quantified, fractionated, and hybridized to the miRNA microarray according to the standard procedures provided by the manufacturer. The labeled RNA was heated to 99 °C for

5 min and then to 45 °C for 5 min. RNA-array hybridization was performed with agitation at 60 rotations per minute for 16–18 h at 48 °C on an Affymetrix® 450 Fluidics Station. The chips were washed and stained using a GeneChip Fluidics Station 450 (Affymetrix, Santa Clara, CA, USA). They were then scanned with an Affymetrix GeneChip Scanner 3000 (Affymetrix, Santa Clara, CA, USA). Signal values were computed using Affymetrix® GeneChip™ Command Console software.

Microarray data processing and normalization

We used a dedicated software tool specialized for such data, which was provided by Affymetrix®. Briefly, raw data were extracted automatically using the Affymetrix data extraction protocol and software provided by Affymetrix GeneChip® Command Console® Software (AGCC). The CEL files import, miRNA level RMA + DABG-All analysis, and export of the results were all performed using Affymetrix® Expression Console™ Software. Array data were filtered by annotated probes for a given species and the data were normalized using AGCC Software. Normalized expression levels across samples are shown in Supplementary Fig. 1.

Differentially expressed miRNA selection

Comparative analysis involving test and control samples was carried out using a fold change and independent *t*-test in which the null hypothesis was that no difference exists between the two groups. False discovery rate (FDR) was controlled by adjusting *p* values using the Benjamini–Hochberg algorithm. All statistical tests and visualization of differentially expressed genes were conducted using the R statistical language v.3.5.2.

Gene ontology and pathway analysis

miRNA-target genes were predicted using the "miRNA-Gene Targets" module of the miRWalk2.0 tool [19, 20]. Pathway and ontology analysis were performed using the clusterProfiler v3.8 R package [21] for target genes of up- and downregulated miRNAs, separately. Network and enrichment analysis using clusterProfiler was performed based on the Hallmark gene set collection in the Molecular Signatures Database (MSigDB, version 6.2). Functional clustering for the identified target genes was performed using the RDAVIDWebService v3.8 R package [22].

Prediction model building and internal validation

To test the predictive ability for lymph node metastasis, classification models were constructed using normalized miRNA expression data. For classification models, eight algorithms including compound covariate predictors, diagonal linear discriminant analysis, 1-nearest neighbor, 3-nearest neighbors, nearest centroid, support vector machine, Bayesian compound covariates, and prediction analysis of microarrays were applied using BRB-Array tools [23]. Briefly, miRNAs exhibiting significantly different levels between M-IMC and N-IMC at $p < 0.001$ by Student's *t* test were used for predictions using the classification models. To evaluate the predictive performance of the classification models, a leave-one-out cross-validation (LOOCV) procedure was used as follows:

Step 1. For the *i*th sample ($I = 1, \ldots, n$), divide the *i*th sample from the whole data as the training set and the remaining $(n - 1)$ patients as the validation set.

Step 2. The classification models were applied to the training set to fit a prediction model.

Step 3. A fitted prediction model was applied to the validation data, and the predicted probabilities were calculated.

Step 4. Repeat steps 1–3 above for all *n* samples.

Step 5. After cross-validation was completed, the predicted probability values of all samples calculated by LOOCV were combined. A single ROC curve was drawn according to Simon et al. [24], and the area under the curve (AUC) was calculated. To remove the overfitting bias of LOOCV as detailed by Simon et al. [24], we calculated a permutation *p* value from 1000 random permutations by each random permutation of the two-class labels for the cross-validated misclassification error rate.

Real-time quantitative reverse transcription polymerase chain reaction (qRT-PCR)

We selected three downregulated miRNAs (miR-106-3p, miR-125a-5p, and miR-486-5p) and three upregulated miRNAs (miR-3175, miR-4742-5p, and miR-4505) for validation using individual TaqMan miRNA assays (Applied Biosystems, Foster city, CA, USA). Tissue RNA containing miRNA was reverse-transcribed into cDNA using multiscribe reverse transcriptase (Applied Biosystems) and a stem-loop primer (Applied Biosystems). qRT-PCR was performed using the TaqMan PCR kit (Applied Biosystems) on an ABI 7500 Realtime PCR system (Applied Biosystems). Each sample was run in triplicate, and miRNA expression levels were normalized to an endogenous control, *RNU6B* (U6). Relative miRNA expression levels were calculated by the comparative threshold cycle (Ct) method using the formula: $2^{-[\Delta Ct(\text{metastatic tumor}) - \Delta Ct(\text{control})]}$.

Immunohistochemistry (IHC)

Immunohistochemical staining was performed with primary antibodies and 4-μm-thick tissue sections of FFPE tissues

using a BenchMark XT® automated immunostainer (Ventana Medical Systems, Tucson, AZ, USA). The following primary antibodies were used: anti-p53 (DO-7, 1:100, Roche Diagnostics, Tucson, AZ, USA), anti-ERK2 (MAPK1, 1:100, Invitrogen, Carlsbad, CA, USA), anti-phospho-p44/42 MAPK (Erk1/2) (Thr202/Tyr204) (D13.14.4E, 1:400, Cell Signaling Technology, Danvers, MA, USA), anti-pS6 (1:300, Cell Signaling Technology), anti-SMAD7 (1:20, Invitrogen), anti-HIF-1-alpha (EP1215Y, 1:100, Abcam, Cambridge, UK), anti-E2F1 (8G9, 1:200, Abcam), and anti-CALD1 (HPA27330, 1:1000, Atlas, Stockholm, Sweden). Tumors showing strong nuclear (for MAPK1, phospho-p44/42 MAPK1, p53, and E2F) or cytoplasmic (for MAPK1, pS6, SMAD7, HIF-1-alpha, and CALD1) staining of >5% of tumor cells were graded 1 (5–25%), 2 (26–50%), or 3 (51–100%), while tumors with no expression or staining < 5% were graded as 0. All IHC slides were independently analyzed by two experienced pathologists (SK and DL).

Statistical analysis

Wilcoxon rank sum tests, unpaired Student's *t* test, Chi-squared test, or Fisher's exact test were performed to compare differences, as and when appropriate. Univariate and multivariate logistic regression analyses were performed to obtain odds ratio for lymph node metastasis. All reported p values are two-sided, and $p < 0.05$ was considered statistically significant. All statistical analyses were performed using R version 3.5.2.

Results

Case selection

Among the 1094 GC samples that were pathologically diagnosed as IMC (T1a), we found 31 patients (2.8%) who revealed lymph node metastasis, with the number of metastatic lymph nodes ranging from 1 to 14. We selected 16 appropriate FFPE tissue samples for microarray analysis from these cases. For comparison, we chose age-, tumor size-, and tumor location-matched N-IMC samples (12 cases), which did not result in metastasis during at least a 5-year follow-up period. Seven normal gastric mucosa tissues which were adjacent to the cancer in the IMC samples were also included. The FFPE samples were all macro-dissected for tumor or normal mucosal areas. Using these samples, total RNA extraction and subsequent miRNA array analysis were performed (Fig. 1). The clinicopathological characteristics of this experimental cohort are summarized in Supplementary Table 1.

Identification of metastasis-related miRNAs in IMCs

miRNA arrays using Affymetrix GeneChip® miRNA 4.0 were used to identify differentially expressed miRNAs in M-IMCs and N-IMCs. We added seven cases of normal gastric mucosa to this array to enable identification of the functional relevance of selected miRNAs. Principal component analysis revealed that cancer and normal samples were separated along the PC1 axis, whereas metastatic- and nonmetastatic cancer samples were differentially located along the PC2 axis (Fig. 2a). Next, we identified 257 small RNAs differentially expressed in normal gastric mucosa and M-IMCs (fold change ≥ 1.5, $p < 0.05$) (Fig. 2b). We then compared M-IMCs with N-IMCs, and found 85 differentially expressed small RNAs (fold change ≥ 1.5, $p < 0.05$). Among these small RNAs, we identified 27 overlapping small RNAs. After excluding six snoRNAs, we finally obtained 21 differentially expressed miRNAs in M-IMCs.

Among these altered miRNAs, ten including miR-628-5p, miR-1587, miR-3175, miR-3620-5p, miR-4459, miR-4505, miR-4507, miR-4720-5p, miR-4742-5p, and miR-6779-5p were significantly upregulated in M-IMCs compared to normal tissue or nonmetastatic cancers (Fig. 2c). Interestingly, most of these miRNAs except miR-3157 and miR-4505 exhibited a stepwise increasing pattern in normal, nonmetastatic, and metastatic cancers. Many of these miRNAs are reported to be upregulated in various cancers, and some of them demonstrated oncogenic properties (Table 1). Eleven miRNAs were significantly downregulated in M-IMCs, and these included miR-106b-3p, miR-125a-5p, miR-151b, miR-181d-5p, miR-486-5p, miR-500a-3p, miR-502-3p, miR-1231, miR-3609, and miR-6831-5p (Fig. 2d). As for miR-125a-5p, miR-151b, miR-181d-5p, and miR-486-5p, expression levels descended stepwise from normal to nonmetastatic cancer to metastatic cancer tissues. Most of the downregulated miRNAs are also reported to be downregulated in other cancers, including GC, and their tumor-suppressive roles have been experimentally confirmed (Table 2). The expression of representative three downregulated (miR-106b-3p, miR-125a-5p, and miR-486-5p) and three upregulated (miR-3175, miR-4742-5p, and miR-4505) miRNAs were validated by using qRT-PCR (Fig. 2e).

Prediction modeling and internal validation

To evaluate whether the miRNAs identified above could be utilized as predictive markers for lymph node metastasis in IMC, we built a prediction model using a machine-learning algorithm to classify M-IMCs and N-IMCs based on miRNAs with significantly increased or decreased expression levels (Fig. 3a). We used the LOOCV procedure for internal

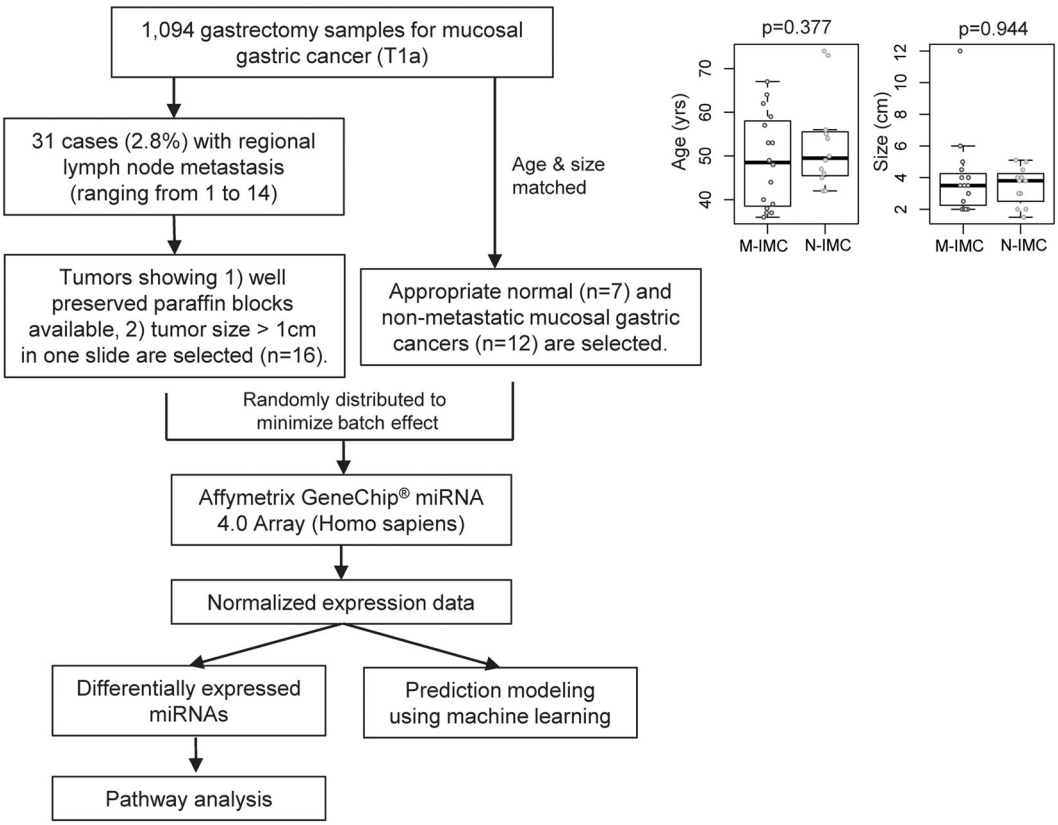

Fig. 1 Overview of the workflow of the study for the identification of specific miRNAs related to lymph node metastasis in intramucosal gastric cancer. Unpaired two-tailed *t* tests were used for statistical analysis of patients' ages and sizes of tumors.

validation because the number of samples was relatively low. Although the classifiers showed various sensitivity, specificity, positive predictive value, and negative predictive value depend on the classifier, the classifiers including diagonal linear discriminant, 1-nearest neighbor, 3-nearest neighbor, and Bayesian compound covariate classifier have p value of <0.05 based on 1000 random permutations, which suggest that the prediction model using the miRNA could be successfully constructed. A LOOCV ROC curve for Bayesian compound covariate predictor (permutated p value = 0.03) exhibited a high AUC value of 0.839 (Fig. 3b). These findings indicated that the miRNA expression profiles we discovered consisting of 21 miRNAs possess value in terms of predicting lymph node metastasis in IMC.

Functional characteristics of metastasis-specific miRNAs

To address the functions of the selected miRNAs, we identified 575 predicted target genes from the 21 selected miRNAs; 384 genes for upregulated miRNAs and 338 genes for downregulated miRNAs were noticed, with 49 overlapping genes (Fig. 4a, Supplementary Table 2). Enriched GO terms related to RNA splicing and development were identified among the upregulated miRNA-target genes. The networks of GO terms derived from downregulated miRNA-target genes were more complex compared to those of upregulated miRNA-target genes, and involved the terms cell cycle, migration, and cellular survival (Fig. 4a, Supplementary Table 3).

Pathway analysis using the Hallmark gene set v.6.2 (Fig. 4b) revealed that the enriched target genes of upregulated miRNAs including *BMPR1A, NCOR2, SKIL, SMAD7, UBE2D3*, and *XIAP* were components of the TGF-β signaling pathway (FDR = 0.031), which is well known to induce tumor cell migration, stimulate epithelial to mesenchymal transition (EMT), promote tumorigenesis, and contribute to chemoresistance [25]. Target genes of downregulated miRNAs were significantly enriched in five distinct signaling pathways with multiple interconnections as follows; E2F targets (*LBR, RAN, CKS2, SRSF2, GINS4, KIF2C, DCK, ESPL1, TFRC, MTHFD2*, and *CDKN1A*; FDR = 0.021), apoptosis (*ANKH, ERBB2, ERBB3, MGMT, CCND1, BCL2L11, IFNGR1, BTG3, SLC20A1*, and *CDKN1A*; FDR = 0.021), hypoxia (*EGFR, CA12, RBPJ, PFKP, F3, ETS1, BCL2, AK4, ENO1*, and *CDKN1A*; FDR = 0.029), mTORC1 signaling (*ACTR2, HSP90B1,*

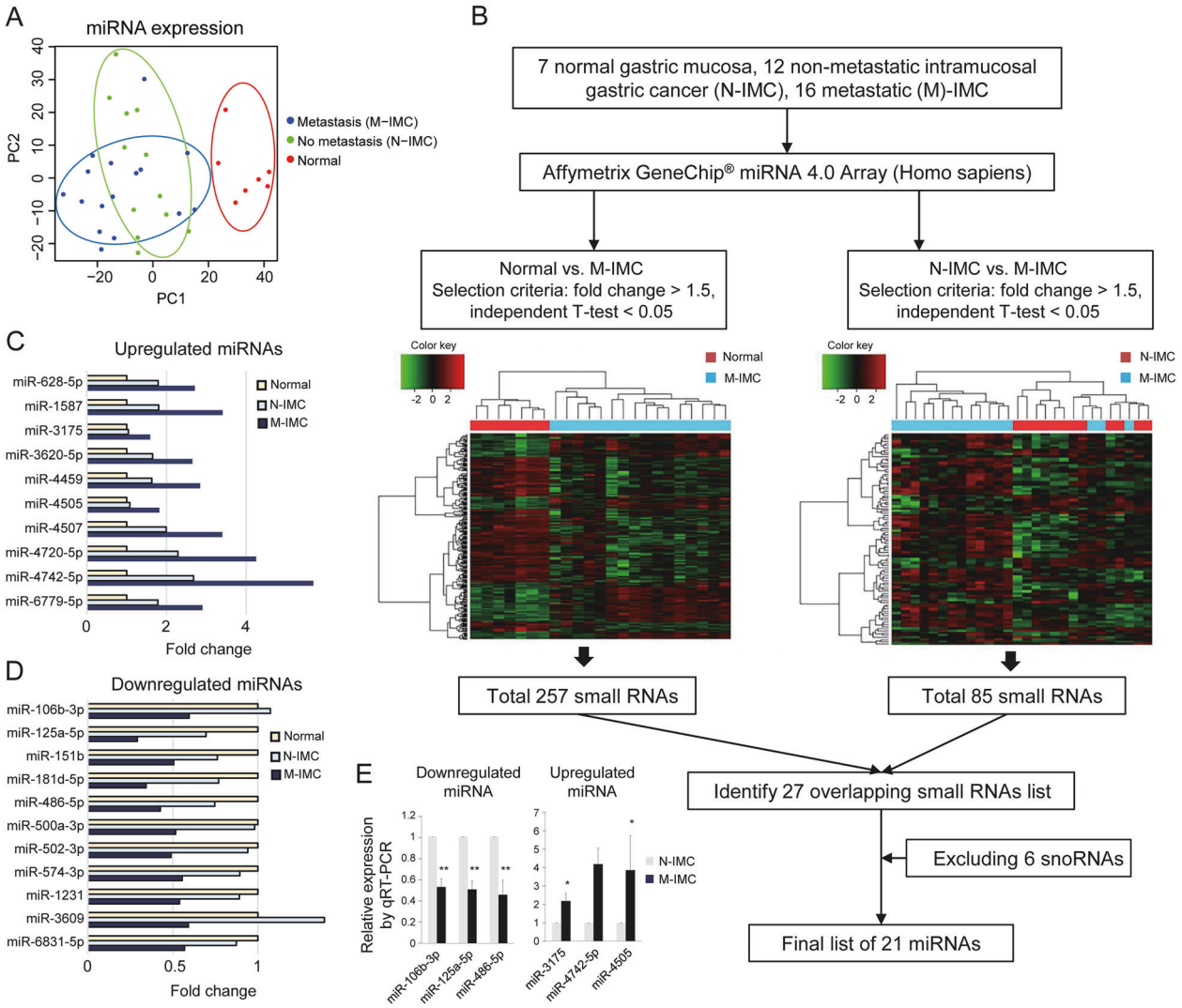

Fig. 2 Differential expression of miRNAs in metastatic- and non-metastatic intramucosal carcinoma (M-IMC and N-IMC). a Principal component analysis of 16 M-IMCs, 12 N-IMCs, and 7 normal gastric mucosal tissues. **b** Workflow of the process for the identification of lymph node metastasis-related miRNAs. **c** List of upregulated miRNAs in M-IMC compared to N-IMC and normal gastric mucosal tissue with relative levels expressed in fold change. **d** Downregulated miRNAs in M-IMC compared to N-IMC and normal gastric mucosal tissue with relative levels expressed in fold change. **e** Experimental validation of altered miRNA expression in M-IMC compared to N-IMC using real-time quantitative reverse transcription polymerase chain reaction (qRT-PCR). All experiments were conducted in triplicate. Data are presented as means ± SD. Unpaired two-tailed *t* tests were used for statistical analysis. $^{**}p < 0.01$ and $^{*}p < 0.05$.

ENO1, AK4, NIBAN1, PSMG1, SCD, TFRC, MTHFD2, and *CDKN1A*; FDR = 0.029), and PI3K-AKT signaling (*MKNK2, VAV3, MAPK1, EGFR, HSP90B1, ACTR2*, and *CDKN1A*; FDR = 0.029). Genes such as *CDN1A, ACTR2*, and *HSP90B1* played a centripetal role linking the enriched signaling pathways. Given that the enriched signaling pathways are critical components of cell cycling or proliferation, we speculate that regulation of tumor cell proliferation by downregulated miRNAs, together with acquisition of EMT and invasive properties from upregulated miRNAs, coordinately promote this early stage of metastasis in GC.

Experimental validation using independent IMC set

We next sought to validate our results using an independent dataset. As M-IMC samples are rare, we collected samples for a validation set from 3 different institutes consisting of 54 metastatic and 54 N-IMCs (Fig. 5a). Then, we performed an miRNA array analysis using these samples. Unfortunately, the independent dataset revealed a wide range of sample quality and severe batch effects on the miRNA array despite normalization (data not shown). Therefore, we performed IHC to validate miRNA signatures in the independent dataset as an alternative option.

Table 1 Upregulated miRNAs in relation to cancer, as sourced from the literature.

miRNA	Relevant cancer	Expression	Source	Note	Ref.
miR-625-5p	Glioblastoma	Up	Serum	Mediates hypoxia-induced migration/invasion	[31]
miR-1587	Glioma	Up	Exosome	Promotes proliferation of glioma cells	[32]
miR-3175	Glioma	Up	Cell line	Promotes proliferation and invasion. Inhibits apoptosis.	[33]
miR-3620-5p	Glioma	Up	Exosome	Promotes proliferation of glioma cells	[32]
miR-4459	Metastatic breast cancer	Up	Tumor	Upregulated in metastatic cancer found in lung	[34]
miR-4505	Colon cancer	Up	Serum	–	[35]
miR-4507	Stage I nasopharyngeal cancer	Up	Tumor	–	[36]
miR-4720-5p	–	–	–	–	–
miR-4742-5p	–	–	–	–	–
miR-6779-5p	–	–	–	–	–

Table 2 Downregulated miRNAs in relation to cancer, as reported in the literature.

miRNA	Relevant cancer	Expression	Source	Note	Ref.
miR-106b-3p	Colorectal cancer	Down	Cell line	Inhibits metastasis	[37]
miR-125a-5p	Head and neck cancer	Down	Tumor	Downregulation is associated with high recurrence and poor prognosis	[28]
	Gastric cancer	Down	Cell line	Inhibits metastasis	[38]
	Breast cancer	Down	Cell line	Inhibits progression	[39]
miR-151b	Thyroid cancer	Down	Serum	–	[40]
miR-181d-5p	Breast and colon cancer	Down	Tumor, cell line	Suppresses cell migration and angiogenesis	[41]
	Non-small cell lung cancer	Down	Tumor, cell line	Suppresses cell proliferation, invasion, and angiogenesis	[42]
miR-486-5p	Non-small cell lung cancer	Down	Tumor, serum, cell line	Suppress cell growth	[43]
	Non-small cell lung cancer	Down	Tumor, cell line	Inhibits cell proliferation and invasion	[44]
miR-500a-3p	Non-small cell lung cancer	Down	Tumor, cell line	Inhibits cell proliferation and invasion	[45]
	Hepatocellular carcinoma	Up	Tumor	Enhances tumorigenicity and stem cell property	[46]
miR-502-3p	Hepatocellular carcinoma	Down	Tumor	Inhibits invasion and metastasis	[47]
miR-574-3p	Breast cancer	Down	Tumor	–	[48]
	Esophageal squamous cell carcinoma	Down	Tumor	Upregulation is associated with non-relapse and favorable prognosis	[49]
miR-1231	Pancreas cancer	Down	Exosome	Inhibits the activity of pancreatic cancer	[50]
	Glioma	Down	Tumor	Suppresses tumor growth	[51]
miR-3609	Chemotherapy-resistant breast cancer	Down	Tumor	Sensitizes cancer cells to adriamycin	[52]
miR-6831-5p	Bladder cancer	Up	Serum	Downregulated in other types of cancer	[53]

We tested antibodies for the direct targets and/or the pathway components of all five miRNA-related pathways found in the experimental set; anti-SMAD7 and anti-CALD1 for TGF-β signaling [26], anti-E2F for E2F targets, anti-p53 for apoptosis, anti-HIF-1α for hypoxia, and anti-MAPK1 (ERK2), anti-phospho-p44/42 MAPK (ERK1/2), and anti-pS6 for PI3K/AKT/mTOR signaling [27]. Among these, we found significantly increased expression of MAPK1, one of the direct targets of downregulated miRNAs, and its activated downstream components (phospho-p44/42 MAPK and pS6, Fig. 5b). The level of SMAD7 expression, a direct target of upregulated miRNAs, showed statistically significant decrease, inferring the action of the miRNAs. In concordance with a previous report [28], the level of p53, a component of apoptotic pathway, was moderately changed, but not significantly so in M-IMC. In this independent dataset, tumor size, invasion depth, and lymphovascular tumor invasion (LVI) were significantly associated with lymph node metastasis ($p < 0.05$ by

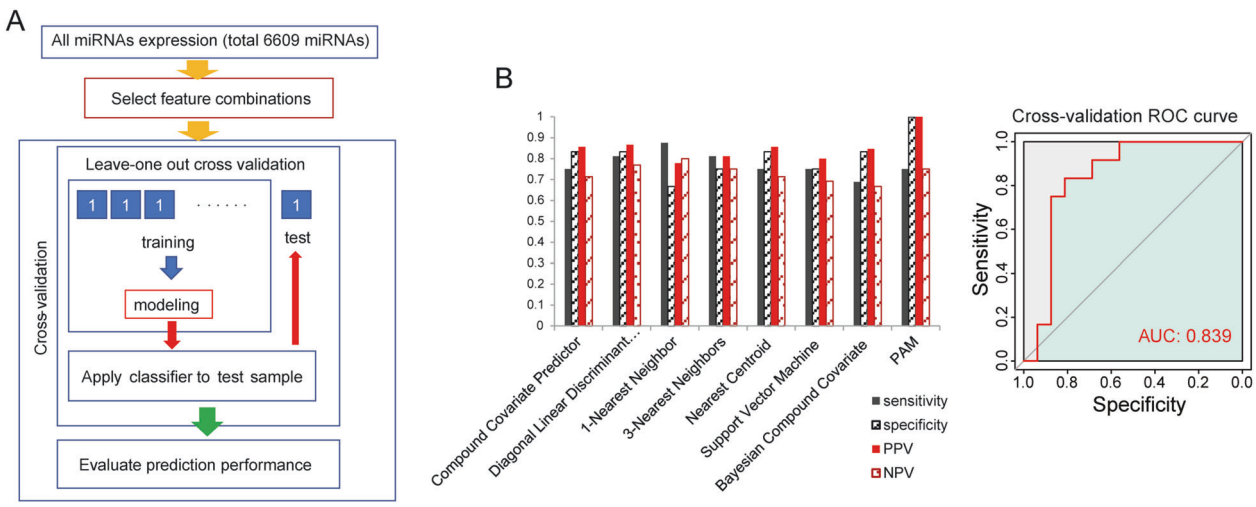

Fig. 3 Predictive model building for lymph node metastasis in intramucosal gastric cancer. a Overview of predictive model building. **b** Performance of the prediction models.

univariate logistic regression analysis, Fig. 5a). Therefore, multivariate logistic regression analysis with these clinical factors (size, depth, and LVI) and the significant target proteins (MAPK1, phospho-p44/42 MAPK, pS6, and SMAD7) was performed and tumor size, LVI, pS6, and SMAD7 were revealed to be independently associated with the lymph node metastasis (Fig. 5c). Representative immunohistochemical staining results for MAPK1, phospho-p44/42 MAPK, pS6, p53, and SMAD7 were shown in Fig. 5d. Other IHC markers did not stain tumor cells reliably; no nuclear staining of E2F1 using auto-stainer, unreliable staining of HIF-1α in cancer cells and which was obscured by strong staining of infiltrating neutrophils, and practically no expression of CALD1 on cancer cells despite manipulation of various staining conditions. It seems that aberrantly expressed genes do not invariably coincide with IHC results, as previously indicated [28]. From these validation dataset results, we could conclude that the miRNA signatures identified in this study somehow exert effects on biological functions in M-IMC samples, and that pS6, and SMAD7 are potential biomarkers that can predict metastasis in IMC.

Discussion

Considering that nodal metastasis of IMC is not uncommon and that current complete resection of the primary tumor is the sole treatment option, biological markers that can predict metastatic potential in intramucosal GC would be valuable to determine treatment strategies and application of post-operative therapies. For more than a decade, many studies have attempted to use miRNAs as markers predicting prognosis in various cancer types, including GC [16, 17]. However, specific miRNA signatures related to metastasis in intramucosal GC have never been investigated.

In this study, we identified the expression of 21 miRNAs, including 10 upregulated miRNAs (miR-628-5p, miR-1587, miR-3175, miR-3620-5p, miR-4459, miR-4505, miR-4507, miR-4720-5p, miR-4742-5p, and miR-6779-5p) and 11 downregulated miRNAs (miR-106b-3p, miR-125a-5p, miR-151b, miR-181d-5p, miR-486-5p, miR-500a-3p, miR-502-3p, miR-574-3p, miR-1231, miR-3609, and miR-6831-5p), which were significantly altered in M-IMCs compared to N-IMCs and nonneoplastic gastric tissues. The majority of these miRNAs are known to be related to tumorigenesis in various types of cancers, and we identified three additional novel miRNAs (miR-4720-5p, miR-4742-5p, and miR-6779-5p) in the context of cancer metastasis. In fact, our group is investigating the specific roles of these novel miRNAs and the preliminary results are promising. Using a machine-learning algorithm, we demonstrated that the identified miRNA signature consisting of 21 miRNAs had considerable value in predicting metastasis in IMCs, suggesting its potential use as a biomarker. However, in order to obtain more reliable results by machine-learning algorithms, a large number of qualified samples is necessary. Due to the difficulty in acquiring miRNAs from tumor samples, only a few studies have conducted external validation only using limited samples [16–18]. When it comes to IMC, this is even more challenging due to its rarity and low tumor volume. Furthermore, as samples from different institutions showed a wide range of sample quality, for miRNA analysis, quality control seems to be critical for the actual utilization of a miRNA signature in clinical settings.

Here, the discovered miRNAs are known to either promote cancer cell proliferation or enhance invasion/metastasis in terms of their mode of action. For example, the upregulated

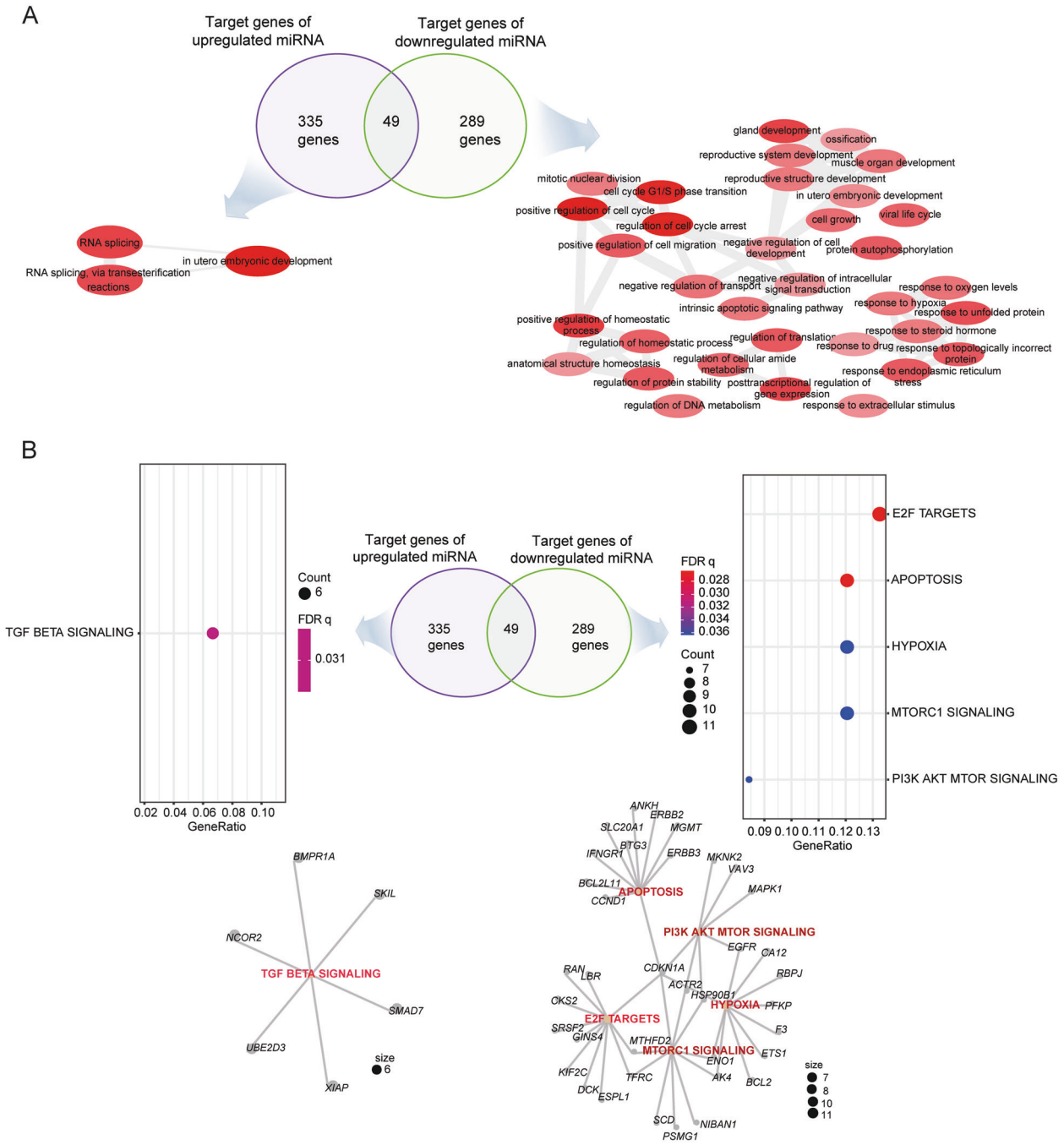

Fig. 4 Gene ontology and pathway analysis for metastasis-related miRNAs. a Gene ontology term enrichment for predicted target genes for upregulated and downregulated miRNAs. **b** Pathway analysis for predicted target genes for upregulated miRNAs and downregulated miRNAs.

miRNAs consisted of miRNAs related to either cellular proliferation (miR-1587, miR-3175, and miR-3620-5p) or invasion/metastasis (miR-628-5p, miR-3175, and miR-4459) (Table 1). In the same manner, the downregulated miRNAs were composed of three miRNAs in relation to proliferation (miR-486-5p, miR-500a-3p, and miR-1231) and six miRNAs to invasion/metastasis (miR-181d-5p, miR-500a-3p, miR-502-3p, miR-106b-3p, miR-125a-5p, and miR-502-3p) (Table 2). Although upregulated and downregulated miRNA groups contain the same components of these two functional categories, it is intriguing that the upregulated miRNAs more closely represent migration or invasion phenotypes mainly driven by TGF-β signaling, whereas the downregulated miRNAs showed greater enrichment in proliferation phenotypes, largely via E2F and AKT/mTOR signaling pathways. Another noticeable finding was that most miRNAs we

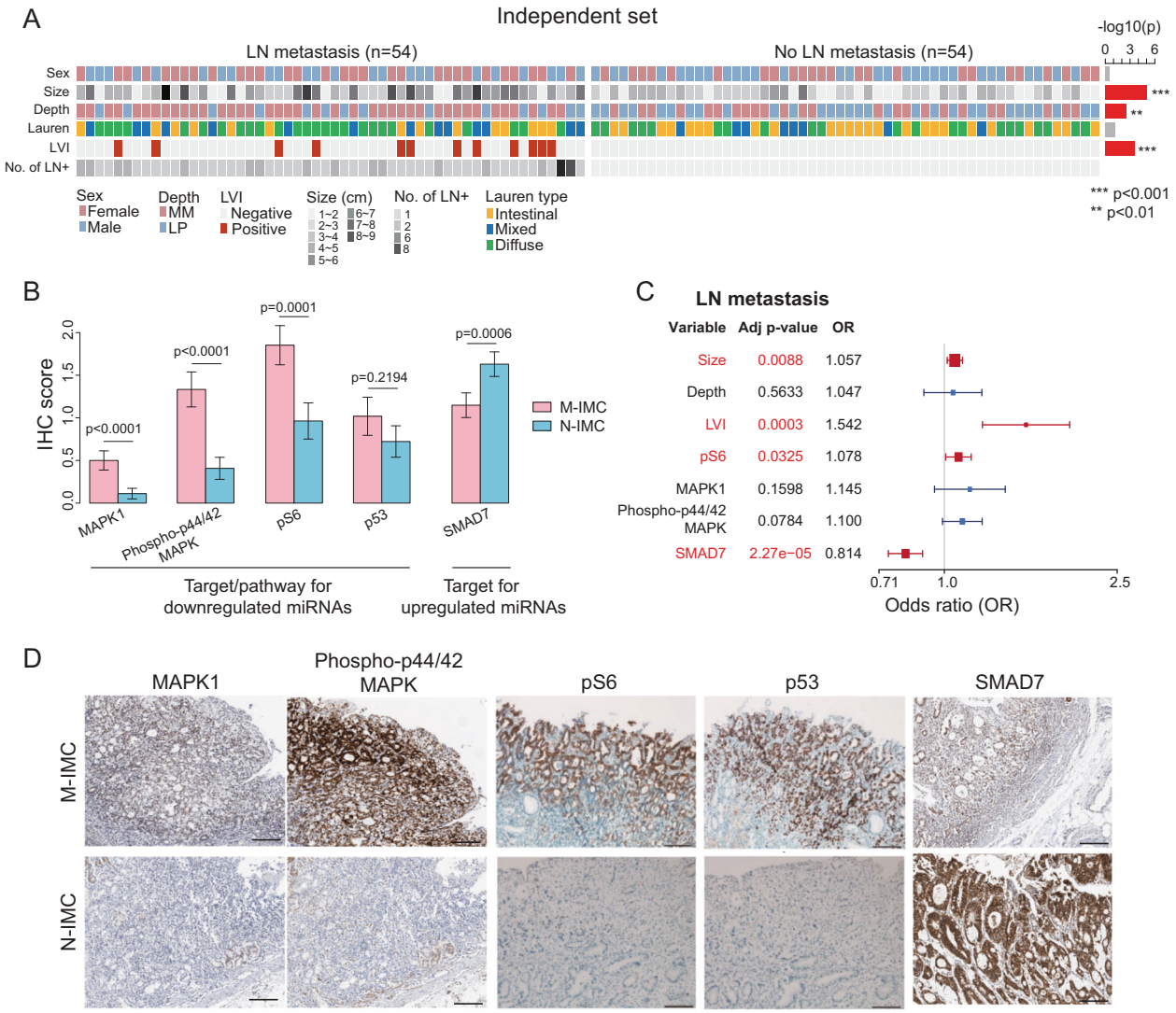

Fig. 5 Analysis of clinicopathological characteristics and experimental validation of metastatic intramucosal gastric cancer using an independent dataset. a Clinicopathological characteristics of an independent sample set composed of 54 M-IMCs and 54 N-IMCs from three different institutes with statistical analysis. LN lymph node, LVI lymphovascular invasion, MM muscularis mucosa, LP lamina propria. Univariate logistic regression analyses were used. ***$p < 0.001$ and **$p < 0.01$. **b** Comparisons of the protein expression of MAPK1 and the pathway proteins (phospho-p44/42 MAPK and pS6), p53, and SMAD7 between M-IMC group and N-IMC group analyzed by immunohistochemical staining (IMC) score. Data are presented as means ± SD. Wilcoxon rank sum tests were used for statistical analysis. **c** Odds ratio of clinicopathological characteristics and IHC results in M-IMC compared to N-IMC. A multivariate logistic regression analysis was used. **d** Representative IHC images of MAPK1, phosho-p44/42 MAPK, pS6, p53, and SMAD7 for M-IMCs and N-IMCs. Scale bar = 200 μm.

identified exhibited stepwise increases or decreases from nonneoplastic tissue to N-IMC to M-IMC. This implies that similar biological mechanisms may be utilized in the process of metastasis as well as in cancer development; only those are intensified in the metastatic process. In this aspect, setting an appropriate threshold for each miRNA in order to distinguish M-IMC from N-IMC is worth pursuing and should be investigated in the future.

In the present study, upregulated or downregulated miRNAs shared 49 common target genes, and this suggested that miRNAs involving the metastasis of intramucosal GC dynamically regulate the expression of cancer-related genes in a complicated manner. This complex genetic regulation cannot be fully explained by conventional sequence-specific suppression or promotion of target genes, but, instead, may be explained, at least in part, by the more sophisticated epigenetic silencing of miRNAs with tumor suppressor features. In fact, a miRNA DNA methylation signature has been reported to be linked to metastasis in various cancer types, including GC [29, 30]. In this regard, epigenetic alterations to miRNAs need to be investigated in metastatic intramucosal GC.

In summary, for the first time, we identified a novel miRNA signature related to metastatic intramucosal GC, which provides insights into the biological mechanisms involved in the development of metastasis at this early stage of disease. Based on this signature, we generated a metastasis prediction model using a machine-learning algorithm and demonstrated potential usage of this signature for prediction of metastasis in IMC. Furthermore, we suggested immunohistochemical markers for improved means to distinguish M-IMC from N-IMC, and this may guide treatment strategies for in patients with IMC in the future.

Acknowledgements This research was supported by the Basic Science Research Program through the National Research Foundation (NRF), funded by the Ministry of Science and ICT (2017R1C1B2003970), Republic of Korea.

Author contributions DL designed the study and supervised the entire process. KWC and COS analyzed and interpreted miRNA expression data. WJB performed qRT-PCR. JMA organized sample data. J-HH and K-MK provided FFPE tumor samples. SK and DL reviewed the tissue slides and performed IHC. SK, COS, and DL wrote the manuscript. All authors were involved in critical review and discussion of this manuscript.

Compliance with ethical standards

Conflict of interest The authors declare that there are no conflicts of interest.

Publisher's note Springer Nature remains neutral with regard to jurisdictional claims in published maps and institutional affiliations.

References

1. Angeles-Angeles A, Candanedo-Gonzalez F, Gamboa-Dominguez A, Larriva-Sahd J. A clinicopathologic variant of intramucosal early gastric cancer with widespread dissemination: report of three cases. J Clin Gastroenterol. 1998;27:173–7.
2. Hanaoka N, Tanabe S, Higuchi K, Sasaki T, Nakatani K, Ishido K, et al. A rare case of histologically mixed-type intramucosal gastric cancer accompanied by nodal recurrence and liver metastasis after endoscopic submucosal dissection. Gastrointest Endosc. 2009;69:588–90.
3. Song SY, Park S, Kim S, Son HJ, Rhee JC. Characteristics of intramucosal gastric carcinoma with lymph node metastatic disease. Histopathology. 2004;44:437–44.
4. Lee D, Kim YC, Lee KM, Yoon JK, Kim YB. MET-amplified intramucosal gastric cancer widely metastatic after complete endoscopic submucosal dissection. Cancer Res Treat. 2015;47:120–5.
5. Korenaga D, Haraguchi M, Tsujitani S, Okamura T, Tamada R, Sugimachi K. Clinicopathological features of mucosal carcinoma of the stomach with lymph node metastasis in eleven patients. Br J Surg. 1986;73:431–3.
6. Yamao T, Shirao K, Ono H, Kondo H, Saito D, Yamaguchi H, et al. Risk factors for lymph node metastasis from intramucosal gastric carcinoma. Cancer. 1996;77:602–6.
7. Lee SH, Choi CW, Kim SJ, Choi CI, Kim DH, Jeon TY, et al. Risk factors for lymph node metastasis in mucosal gastric cancer and re-evaluation of endoscopic submucosal dissection. Ann Surg Treat Res. 2016;91:118–26.
8. Wang H, Wei XZ, Fu CG, Zhao RH, Cao FA. Patterns of lymph node metastasis are different in colon and rectal carcinomas. World J Gastroenterol. 2010;16:5375–9.
9. Zhao YX, Liu YR, Xie S, Jiang YZ, Shao ZM. A nomogram predicting lymph node metastasis in T1 breast cancer based on the surveillance, epidemiology, and end results program. J Cancer. 2019;10:2443–9.
10. Cancer Genome Atlas Research N. Comprehensive molecular characterization of gastric adenocarcinoma. Nature. 2014;513:202–9.
11. Choi JH, Kim YB, Ahn JM, Kim MJ, Bae WJ, Han SU, et al. Identification of genomic aberrations associated with lymph node metastasis in diffuse-type gastric cancer. Exp Mol Med. 2018;50:6.
12. Calin GA, Ferracin M, Cimmino A, Di Leva G, Shimizu M, Wojcik SE, et al. A MicroRNA signature associated with prognosis and progression in chronic lymphocytic leukemia. N Engl J Med. 2005;353:1793–801.
13. Yanaihara N, Caplen N, Bowman E, Seike M, Kumamoto K, Yi M, et al. Unique microRNA molecular profiles in lung cancer diagnosis and prognosis. Cancer Cell. 2006;9:189–98.
14. Bloomston M, Frankel WL, Petrocca F, Volinia S, Alder H, Hagan JP, et al. MicroRNA expression patterns to differentiate pancreatic adenocarcinoma from normal pancreas and chronic pancreatitis. JAMA. 2007;297:1901–8.
15. Garzon R, Volinia S, Liu CG, Fernandez-Cymering C, Palumbo T, Pichiorri F, et al. MicroRNA signatures associated with cytogenetics and prognosis in acute myeloid leukemia. Blood. 2008;111:3183–9.
16. Hao NB, He YF, Li XQ, Wang K, Wang RL. The role of miRNA and lncRNA in gastric cancer. Oncotarget. 2017;8:81572–82.
17. Li X, Zhang Y, Zhang Y, Ding J, Wu K, Fan D. Survival prediction of gastric cancer by a seven-microRNA signature. Gut. 2010;59:579–85.
18. Hwang J, Min BH, Jang J, Kang SY, Bae H, Jang SS, et al. MicroRNA expression profiles in gastric carcinogenesis. Sci Rep. 2018;8:14393.
19. Dweep H, Gretz N. miRWalk2.0: a comprehensive atlas of microRNA-target interactions. Nat Methods. 2015;12:697.
20. Dweep H, Sticht C, Pandey P, Gretz N. miRWalk-database: prediction of possible miRNA binding sites by "walking" the genes of three genomes. J Biomed Inform. 2011;44:839–47.
21. Yu G, Wang LG, Han Y, He QY. clusterProfiler: an R package for comparing biological themes among gene clusters. OMICS. 2012;16:284–7.
22. Fresno C, Fernandez EA. RDAVIDWebService: a versatile R interface to DAVID. Bioinformatics. 2013;29:2810–1.
23. Simon R, Lam A, Li MC, Ngan M, Menenzes S, Zhao Y. Analysis of gene expression data using BRB-ArrayTools. Cancer Informat. 2007;3:11–7.
24. Simon RM, Subramanian J, Li MC, Menezes S. Using cross-validation to evaluate predictive accuracy of survival risk classifiers based on high-dimensional data. Brief Bioinformat. 2011;12:203–14.
25. Colak S, Ten Dijke P. Targeting TGF-beta Signaling in. Cancer Trends Cancer. 2017;3:56–71.
26. Tauriello DVF, Palomo-Ponce S, Stork D, Berenguer-Llergo A, Badia-Ramentol J, Iglesias M, et al. TGFbeta drives immune evasion in genetically reconstituted colon cancer metastasis. Nature. 2018;554:538–43.
27. Kim YB, Ham IH, Hur H, Lee D. Various ARID1A expression patterns and their clinical significance in gastric cancers. Hum Pathol. 2016;49:61–70.

28. Nishida N, Mimori K, Fabbri M, Yokobori T, Sudo T, Tanaka F, et al. MicroRNA-125a-5p is an independent prognostic factor in gastric cancer and inhibits the proliferation of human gastric cancer cells in combination with trastuzumab. Clin Cancer Res. 2011;17:2725–33.
29. Lujambio A, Calin GA, Villanueva A, Ropero S, Sanchez-Cespedes M, Blanco D, et al. A microRNA DNA methylation signature for human cancer metastasis. Proc Natl Acad Sci USA. 2008;105:13556–61.
30. Nicoloso MS, Spizzo R, Shimizu M, Rossi S, Calin GA. MicroRNAs-the micro steering wheel of tumour metastases. Nat Rev Cancer. 2009;9:293–302.
31. Dong L, Li Y, Han C, Wang X, She L, Zhang H. miRNA microarray reveals specific expression in the peripheral blood of glioblastoma patients. Int J Oncol. 2014;45:746–56.
32. Figueroa J, Phillips LM, Shahar T, Hossain A, Gumin J, Kim H. Exosomes from glioma-associated mesenchymal stem cells increase the tumorigenicity of glioma stem-like cells via transfer of miR-1587. Cancer Res. 2017;77:5808–19.
33. Han L, Liu D, Li Z, Tian N, Han Z, Wang G, et al. HOXB1 is a tumor suppressor gene regulated by miR-3175 in glioma. PLoS ONE. 2015;10:e0142387.
34. Martinez-Gutierrez AD, Catalan OM, Vazquez-Romo R, Porras Reyes FI, Alvarado-Miranda A, Lara Medina F, et al. miRNA profile obtained by nextgeneration sequencing in metastatic breast cancer patients is able to predict the response to systemic treatments. Int J Mol Med. 2019;44:1267–80.
35. Wang YN, Chen ZH, Chen WC. Novel circulating microRNAs expression profile in colon cancer: a pilot study. Eur J Med Res. 2017;22:51.
36. Li S, Hang L, Ma Y, Wu C. Distinctive microRNA expression in early stage nasopharyngeal carcinoma patients. J Cell Mol Med. 2016;20:2259–68.
37. Ni S, Weng W, Xu M, Wang Q, Tan C, Sun H, et al. miR-106b-5p inhibits the invasion and metastasis of colorectal cancer by targeting CTSA. Onco Targets Ther. 2018;11:3835–45.
38. Cao Y, Tan S, Tu Y, Zhang G, Liu Y, Li D, et al. MicroRNA-125a-5p inhibits invasion and metastasis of gastric cancer cells by targeting BRMS1 expression. Oncol Lett. 2018;15:5119–30.
39. Yan L, Yu MC, Gao GL, Liang HW, Zhou XY, Zhu ZT, et al. MiR-125a-5p functions as a tumour suppressor in breast cancer by downregulating BAP1. J Cell Biochem. 2018;119:8773–83.
40. Hu Y, Wang H, Chen E, Xu Z, Chen B, Lu G. Candidate microRNAs as biomarkers of thyroid carcinoma: a systematic review, meta-analysis, and experimental validation. Cancer Med. 2016;5:2602–14.
41. Li Y, Kuscu C, Banach A, Zhang Q, Pulkoski-Gross A, Kim D, et al. miR-181a-5p inhibits cancer cell migration and angiogenesis via downregulation of matrix metalloproteinase-14. Cancer Res. 2015;75:2674–85.
42. Gao LM, Zheng Y, Wang P, Zheng L, Zhang WL, Di Y, et al. Tumor-suppressive effects of microRNA-181d-5p on non-small-cell lung cancer through the CDKN3-mediated Akt signaling pathway in vivo and in vitro. Am J Physiol Lung Cell Mol Physiol. 2019;316:L918–L33.
43. Tian F, Wang J, Ouyang T, Lu N, Lu J, Shen Y, et al. MiR-486-5p serves as a good biomarker in nonsmall cell lung cancer and suppresses cell growth with the involvement of a target PIK3R1. Front Genet. 2019;10:688.
44. Yu S, Geng S, Hu Y. miR-486-5p inhibits cell proliferation and invasion through repressing GAB2 in non-small cell lung cancer. Oncol Lett. 2018;16:3525–30.
45. Liao XH, Xie Z, Guan CN. MiRNA-500a-3p inhibits cell proliferation and invasion by targeting lymphocyte antigen 6 complex locus K (LY6K) in human non-small cell lung cancer. Neoplasma. 2018;65:673–82.
46. Jiang C, Long J, Liu B, Xu M, Wang W, Xie X, et al. miR-500a-3p promotes cancer stem cells properties via STAT3 pathway in human hepatocellular carcinoma. J Exp Clin Cancer Res. 2017;36:99.
47. Jin H, Yu M, Lin Y, Hou B, Wu Z, Li Z, et al. MiR-502-3P suppresses cell proliferation, migration, and invasion in hepatocellular carcinoma by targeting SET. Onco Targets Ther. 2016;9:3281–9.
48. Ujihira T, Ikeda K, Suzuki T, Yamaga R, Sato W, Horie-Inoue K, et al. MicroRNA-574-3p, identified by microRNA library-based functional screening, modulates tamoxifen response in breast cancer. Sci Rep. 2015;5:7641.
49. Okumura T, Kojima H, Miwa T, Sekine S, Hashimoto I, Hojo S, et al. The expression of microRNA 574-3p as a predictor of postoperative outcome in patients with esophageal squamous cell carcinoma. World J Surg Oncol. 2016;14:228.
50. Shang S, Wang J, Chen S, Tian R, Zeng H, Wang L, et al. Exosomal miRNA-1231 derived from bone marrow mesenchymal stem cells inhibits the activity of pancreatic cancer. Cancer Med. 2019;8:7728–40.
51. Zhang J, Zhang J, Qiu W, Zhang J, Li Y, Kong E, et al. MicroRNA-1231 exerts a tumor suppressor role through regulating the EGFR/PI3K/AKT axis in glioma. J Neurooncol. 2018;139:547–62.
52. Li D, Wang X, Yang M, Kan Q, Duan Z. miR3609 sensitizes breast cancer cells to adriamycin by blocking the programmed death-ligand 1 immune checkpoint. Exp Cell Res. 2019;380:20–8.
53. Usuba W, Urabe F, Yamamoto Y, Matsuzaki J, Sasaki H, Ichikawa M, et al. Circulating miRNA panels for specific and early detection in bladder cancer. Cancer Sci. 2019;110:408–19.